Excited-quark and -lepton production at hadron colliders

U. Baur
Physics Department, University of Wisconsin, Madison, Wisconsin 53706

M. Spira and P. M. Zerwas
Institut fur Theoretische Physik, Rheinisch-Westfälische Technische Hochschule Aachen, D-5100 Aachen, Federal Republic of Germany

(Received 29 November 1989)

The existence of excited states is a natural consequence of composite models for quarks and leptons. Production rates and signatures are discussed for hadron colliders presently operating (CERN Super $p\bar{p}$ Synchrotron and Fermilab Tevatron) or under study (CERN Large Hadron Collider and Superconducting Super Collider). Contact interactions may be an important source for excited fermions and could influence the signatures of such particles significantly. Excited quarks could be discovered with masses up to about $\frac{1}{3}-\frac{1}{2}$ of the total collider energy while excited leptons could be accessible up to $\frac{1}{5}-\frac{1}{3}$ of the available energy. Large lepton yields are expected if quarks and leptons share common subconstituents.

I. INTRODUCTION

The proliferation of quarks and leptons is often taken as a sign for a possible substructure of these particles. The most convincing evidence for a substructure of quarks and leptons would be the discovery of excited states towering over the leptonic and quark ground states:[1-11]

$$l, l^*, l^{**}, \ldots, \quad q, q^*, q^{**}, \ldots .$$

The masses m^* of excited fermions are generally expected to be at least of the order of a few hundred GeV. According to present experimental constraints from static lepton properties, such as $(g-2)_{e,\mu}$ and the estimate of quark and lepton radii from high-energy e^+e^- and hadronic collisions, the substructure scale Λ cannot be much smaller than 1 TeV (Ref. 12) and excited states should not be much lighter than Λ. It is therefore not very surprising that searches for excited fermions have been unsuccessful so far.

With higher center-of-mass energies available in $p\bar{p}$ collisions at the Fermilab Tevatron and the realistic possibility of multi-TeV pp colliders going into operation within the next decade, the prospects for finding the lowest excited states of the spectrum become much better, if such particles exist at all. This has motivated us to reexamine excited fermion production at hadron colliders, and to estimate discovery limits for the CERN $p\bar{p}$ collider, the Fermilab Tevatron, as well as the pp colliders, the CERN Large Hadron Collider (LHC) and the Superconducting Super Collider (SSC). The extrapolation to energies beyond the reach of the SSC follows simple scaling laws.[13] In particular we shall consider excited fermion production via contact interactions which so far has not been studied in detail. [Excited-quark production via quark-gluon fusion has been discussed already in earlier papers (see, e.g., Refs. 3–5). However, in order to present a complete and coherent analysis we discuss this mechanism also here in some detail.] Contact interactions may be an important source for excited fermion production and yield new (leptonic) signatures for such states. Since a detailed theoretical approach to preon dynamics is lacking, we shall focus on representative examples illuminating the gross features of excited states.

II. THE PHYSICAL SETUP

Spin and isospin of the excited fermions will be set to $\frac{1}{2}$ in order to limit the number of parameters in this study. The assignment of left- and right-handed components to isodoublets, e.g., for the first generation,

$$\begin{pmatrix} \nu_e \\ e^- \end{pmatrix}_L, \quad e_R^- \begin{pmatrix} \nu_e^* \\ e^{*-} \end{pmatrix}_L, \quad \begin{pmatrix} \nu_e^* \\ e^{*-} \end{pmatrix}_R ,$$

$$\begin{pmatrix} u \\ d \end{pmatrix}_L, \quad u_R \begin{pmatrix} u^* \\ d^* \end{pmatrix}_L, \quad \begin{pmatrix} u^* \\ d^* \end{pmatrix}_R ,$$

allows for nonzero masses prior to SU(2)×U(1)-symmetry breaking, and it protects $(g-2)_l$ quadratically in the mass ratio $(m_l/m^*)^2$ $(l=e,\mu)$.[14] This could also be achieved by assigning all excited states to isosinglets. Such a case can easily be treated in analogy to the doublet assignment so that it need not be elaborated in detail here.

The coupling of excited fermion states $f^*=\nu_e^*, \ldots, d^*$ to gluons, γ, $W^\pm$ and Z [see Fig. 1(a)] is vectorlike:

$$\mathcal{L}_{\text{gauge}} = \bar{f}^* \gamma^\mu \left(g_s \frac{\lambda^a}{2} G_\mu^a + g \frac{\tau}{2} \cdot \mathbf{W}_\mu + g' \frac{Y}{2} B_\mu \right) f^* . \qquad (1)$$

The weak hypercharge Y of the excited states is -1 and $\frac{1}{3}$ in the lepton and quark sector, respectively; g_s, $g=e/\sin\theta_W$ and $g'=e/\cos\theta_W$ are the strong and elec-

troweak gauge couplings. G_μ^a, $\mathbf{W}_\mu$, and B_μ describe the gluon, the SU(2), and the U(1) gauge fields. Each of the vertices will in general be modified by form factors.[14,15]

Gauge bosons can also mediate transitions between ordinary (left-handed) and excited (right-handed) fermions [see Fig. 1(b)]. The form of the effective Lagrangian describing these transitions is uniquely fixed by gauge invariance to be of magnetic-moment type

$$\mathcal{L}_{\text{trans}}=\frac{1}{2\Lambda}\bar{f}_R^*\sigma^{\mu\nu}\left[g_s f_s\frac{\lambda^a}{2}G_{\mu\nu}^a+gf\frac{\tau}{2}\cdot\mathbf{W}_{\mu\nu}+g'f'\frac{Y}{2}B_{\mu\nu}\right]f_L+\text{H.c.}\ , \tag{2}$$

where $G_{\mu\nu}^a$, $\mathbf{W}_{\mu\nu}$, and $B_{\mu\nu}$ are the field-strength tensors of the gluon, the SU(2) and the U(1) gauge fields. f_s, f, and f' are parameters determined by the composite dynamics. Naively one would expect them to be all of order 1. Higher-dimensional operators in the full effective Lagrangian can be incorporated by changing the f's to form factors $f_s(q^2)$, $f(q^2)$, and $f'(q^2)$.[9] Λ, finally, is the compositeness scale.

Excited fermions may also couple to ordinary quarks and leptons via contact interactions resulting from novel strong preon interactions [see Fig. 1(c)]. For energies below the compositeness scale Λ they can be described by an effective four-fermion Lagrangian of the type[5,8]

$$\mathcal{L}_{\text{contact}}=\frac{g_*^2}{\Lambda^2}\frac{1}{2}j^\mu j_\mu \tag{3}$$

with

$$j_\mu=\eta_L\bar{f}_L\gamma_\mu f_L+\eta_L'\bar{f}_L^*\gamma_\mu f_L^*+\eta_L''\bar{f}_L^*\gamma_\mu f_L+\text{H.c.}+(L\to R)\ . \tag{4}$$

In the following g_*^2 is chosen to be equal to 4π and the η factors of left-handed currents equal to one, while right-handed currents, for simplicity, will be neglected.

For $\hat{s}^{1/2}\gtrsim\Lambda$, the pointlike hard coupling equation (3) must be dissolved in order to damp the rise of the cross sections with energy that is induced by a four-fermion coupling. Furthermore, higher-dimensional contact terms are expected to become important. In our calculations we shall always use the effective Lagrangian of Eq. (3). This ansatz should be sufficient to provide a *rough estimate* of how preon interchange will affect the widths of excited fermionic states and their production cross sections.

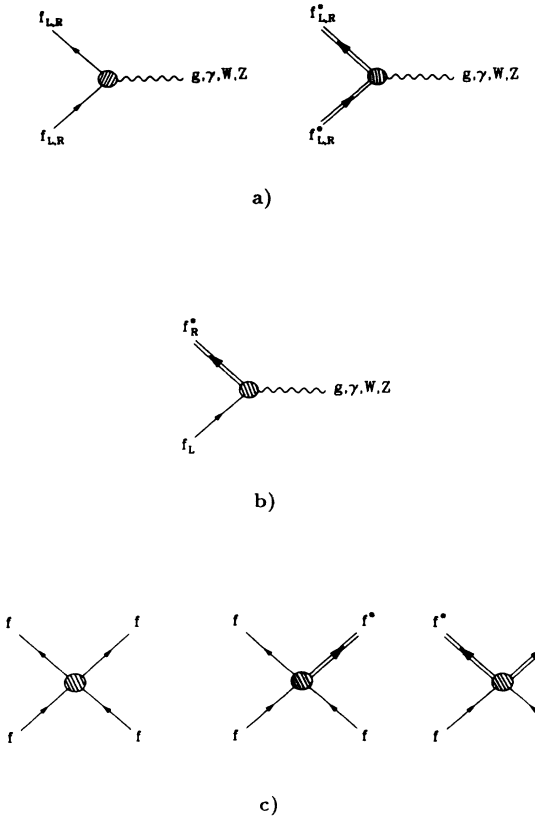

FIG. 1. (a) Gauge interactions of light and excited fermions. The W boson couples to left- and right-handed excited fermions, but only to left-handed ordinary fermions. (b) Transitions between ordinary and excited fermions via gauge-boson emission. (c) Contact interactions.

III. THE WIDTHS OF EXCITED QUARKS AND LEPTONS

Heavy excited fermions will decay into light fermions plus gauge bosons, but also, through preon-pair creation, into bunches of quarks and leptons. Assuming $m^*>m_{W,Z}$ and neglecting ordinary quark masses, the partial widths for the various electroweak decay channels are ($V=W,Z$) (Refs. 4 and 5)

$$\Gamma(f^*\to f\gamma)=\frac{1}{4}\alpha f_\gamma^2\frac{m^{*3}}{\Lambda^2}\ , \tag{5}$$

$$\Gamma(f^*\to fV)=\frac{1}{8}\frac{g_V^2}{4\pi}f_V^2\frac{m^{*3}}{\Lambda^2}\left[1-\frac{m_V^2}{m^{*2}}\right]^2\left[2+\frac{m_V^2}{m^{*2}}\right] \tag{6}$$

with

$$f_\gamma=fT_3+f'\frac{Y}{2}\ , \tag{7}$$

$$f_Z=fT_3\cos^2\theta_W-f'\frac{Y}{2}\sin^2\theta_W\ , \tag{8}$$

$$f_W=\frac{f}{\sqrt{2}}\ . \tag{9}$$

Here, T_3 denotes the third component of the weak isospin of f^*, and $g_W=e/\sin\theta_W$ ($e=\sqrt{4\pi\alpha}$) and $g_Z=g_W/\cos\theta_W$ are the standard-model W and Z coupling constants. For the decay of excited quarks into ordinary quarks and gluons one finds

$$\Gamma(q^*\to qg)=\frac{1}{3}\alpha_s f_s^2\frac{m^{*3}}{\Lambda^2}\ . \tag{10}$$

The widths for decays into gauge particles are fairly small; taking for illustration $m^*=\Lambda$, one finds the values

TABLE I. Decay widths of excited fermions into ordinary fermions and gauge bosons for $m^*=\Lambda$ and $f_s=f=f'=1$.

f^*	$\sum_V \Gamma(f^*\to fV)/m^*$
ν^*	6.5×10^{-3}
e^*	6.5×10^{-3}
u^*	3.9×10^{-2}
d^*	3.9×10^{-2}

listed in Table I, i.e., approximately 70 GeV for e^* and 400 GeV for q^* if the masses are set to $m^*=10$ TeV and $f_s=f=f'=1$. According to Eq. (10) decays of excited quarks into gauge bosons predominantly yield a quark plus a gluon. Radiative transitions and decays into quarks and a weak boson will typically appear at $O(\alpha/\alpha_s)$, i.e., at the few % level. Excited lepton decays mediated by electroweak interactions mostly result in a W boson and an ordinary lepton. As long as the f^* mass is sufficiently large compared to m_W and m_Z the branching ratios will be insensitive to m^*. The relative gauge branching ratios $B_G=\Gamma(f^*\to fV)/\sum_V \Gamma(f^*\to fV)$ are summarized in Table II.

The widths can however be significantly increased by decays which are mediated by contact interactions. From Eqs. (3) and (4) one obtains

$$\Gamma(f^*\to f+f'\bar{f}')=\frac{m^*}{96\pi}\left[\frac{m^*}{\Lambda}\right]^4 N_c' S' \ . \tag{11}$$

$N_c'=3$ or 1 is the number of colors of the light fermion f', and S' is an additional combinatorical factor:

$S'=1$ for $f\neq f'$,

$S'=\frac{4}{3}$ for $f=f'$ and quarks ,

$S'=2$ for $f=f'$ and leptons .

For three generations and $m^*=\Lambda=10$ TeV, Eq. (11) leads to f^* widths of ~1 TeV, i.e., 10% of the mass of the excited states. This is still in the same ballpark as the gauge decay widths of excited quarks; however, excited lepton states can have a much larger width than predicted by the electroweak decay channels—a natural consequence of the *strong* interactions at the subconstituent level. More details on the total widths and branching ratios are summarized in Table III. Excellent signatures are predicted by the large fraction of decays with leptons in the final state, that are a consequence of the uniform coupling among quarks and leptons through the contact interactions Eq. (3). The relative importance of decays mediated by contact interactions depends, however, rather strongly on the ratio m^*/Λ. This is obvious from Eqs. (5), (6), and (11).

TABLE II. Relative branching ratios $B_G=\Gamma(f^*\to fV)/\sum_V \Gamma(f^*\to fV)$ for decays of excited fermions into gauge bosons for $m^*=\Lambda$, $f_s=f=f'=1$, and $\alpha_s=0.11$.

Decay mode	B_G	Decay mode	B_G
		$e^*\to e\gamma$	0.28
$\nu^*\to\nu Z$	0.39	$e^*\to eZ$	0.11
$\nu^*\to eW$	0.61	$e^*\to\nu W$	0.61
$u^*\to ug$	0.85	$d^*\to dg$	0.85
$u^*\to u\gamma$	0.02	$d^*\to d\gamma$	0.005
$u^*\to uZ$	0.03	$d^*\to dZ$	0.05
$u^*\to dW$	0.10	$d^*\to uW$	0.10

IV. PRODUCTION IN $p\bar{p}$ AND pp COLLISIONS

Excited quarks can be produced in $p\bar{p}$ and pp collisions through a variety of mechanisms. The most obvious reaction is $q^*\bar{q}^*$ pair creation via quark-antiquark annihilation or gluon-gluon fusion.[11] The corresponding cross section can be predicted reliably, yet it turns out to be so small that discriminating the signal from the ordinary QCD and electroweak background processes would be rather difficult. Much more promising are the gluonic excitation of quarks $g+q\to q^*$, and the excitation through contact interactions, e.g., $q\bar{q}\to q\bar{q}^*$ or $q\bar{q}\to q^*\bar{q}^*$. The subsequent decay of excited quarks leads to peaks in the jet-photon invariant-mass spectrum, or in the invariant-mass distributions of jets and jets-plus-lepton pairs. Excited leptons can be produced at hadron colliders either singly, via $q\bar{q}\to l\bar{l}^*$, $l^*\bar{l}$, or pairwise, via $q\bar{q}\to l^*\bar{l}^*$, through contact interactions ($l=e,\nu$). Their decays lead to lepton-photon pairs, or final states consisting of three leptons, or one lepton plus a quark pair. The quark pairs come either from decays into W and Z bosons or from decays mediated by preon contact interactions. The first indication for the production of novel excited fermions thus could be the copious production of leptons—at rates much larger than expected in the framework of the standard model.

A. q^* production via quark-gluon fusion

The cross section for the gluonic excitation of quarks, $qg\to q^*$, at hadron colliders [see Fig. 2(a)] is given by

TABLE III. Decay widths of excited fermions mediated by gauge (G) and contact interactions (CT) for $m^*=\Lambda$ and $f_s=f=f'=1$. The last column gives the percentage of decays leading to at least one lepton in the final state.

f^*	$\Gamma_{\rm tot}/m^*$	$\Gamma_G/\Gamma_{\rm tot}$	$\Gamma_{CT}/\Gamma_{\rm tot}$	Leptonic decays/all
ν^*	8.9×10^{-2}	0.07	0.93	100%
e^*	8.9×10^{-2}	0.07	0.93	100%
u^*	1.2×10^{-1}	0.32	0.68	16.3%
d^*	1.2×10^{-1}	0.32	0.68	16.3%

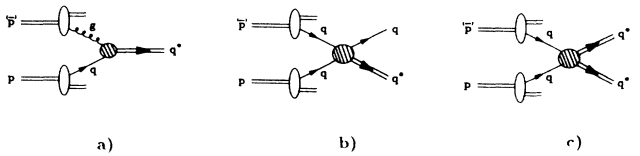

FIG. 2. Generic diagrams contributing to q^* production in hadronic collisions: (a) quark gluon fusion, (b) qq^* production via contact interactions, and (c) q^* pair production via contact interactions.

$$\sigma = \frac{\alpha_s \pi^2}{3\Lambda^2} f_s^2 \tau \frac{d\mathcal{L}^{gq}}{d\tau} \tag{12}$$

with

$$\tau = \frac{m^{*2}}{s} . \tag{13}$$

s is the center-of-mass energy squared and $d\mathcal{L}^{gq}/d\tau$ denotes the quark-gluon luminosity. If gauge interactions are dominating, the signals for singly produced excited quarks are large transverse momentum jj, $j\gamma$, jZ, or jW pairs with an invariant mass peaking at m^*. For jW final states in which the W decays leptonically, the invariant mass can, however, only be determined with a twofold ambiguity, due to the nonobservation of the neutrino.

The jj mass distributions above the QCD background for $p\bar{p}$ collisions at $\sqrt{s}=630$ GeV (S$p\bar{p}$S) and 1.8 TeV (Fermilab Tevatron), and for pp collisions at $\sqrt{s}=16$ TeV (LHC) and 40 TeV (SSC), are shown in Fig. 3 for various values of m^*. For simplicity Λ is identified with m^* and $f_s=f=f'=1$. Gauge interactions are assumed to dominate over contact interactions. Because the masses of excited quarks arise prior to SU(2)×U(1) breaking, members of an excited weak doublet should be nearly degenerate in mass. Furthermore, the q^* charge cannot be determined experimentally at a hadron collider, and we have thus summed up the u^*, d^*, $\bar{u}^*$, and $\bar{d}^*$ rates. The q^* production cross sections are then equal in $p\bar{p}$ and pp collisions.

The parameters used in Fig. 3 and all subsequent figures are $\alpha=\alpha(m_W)=1/128$, $m_W=81$ GeV, $m_Z=92$ GeV, and $\sin^2\theta_W=0.23$. For the parton distributions we used set 1 of Ref. 11. The scale Q^2 at which the structure functions are evaluated is chosen to be the center-of-mass energy squared, $\hat{s}$, unless stated otherwise. To roughly

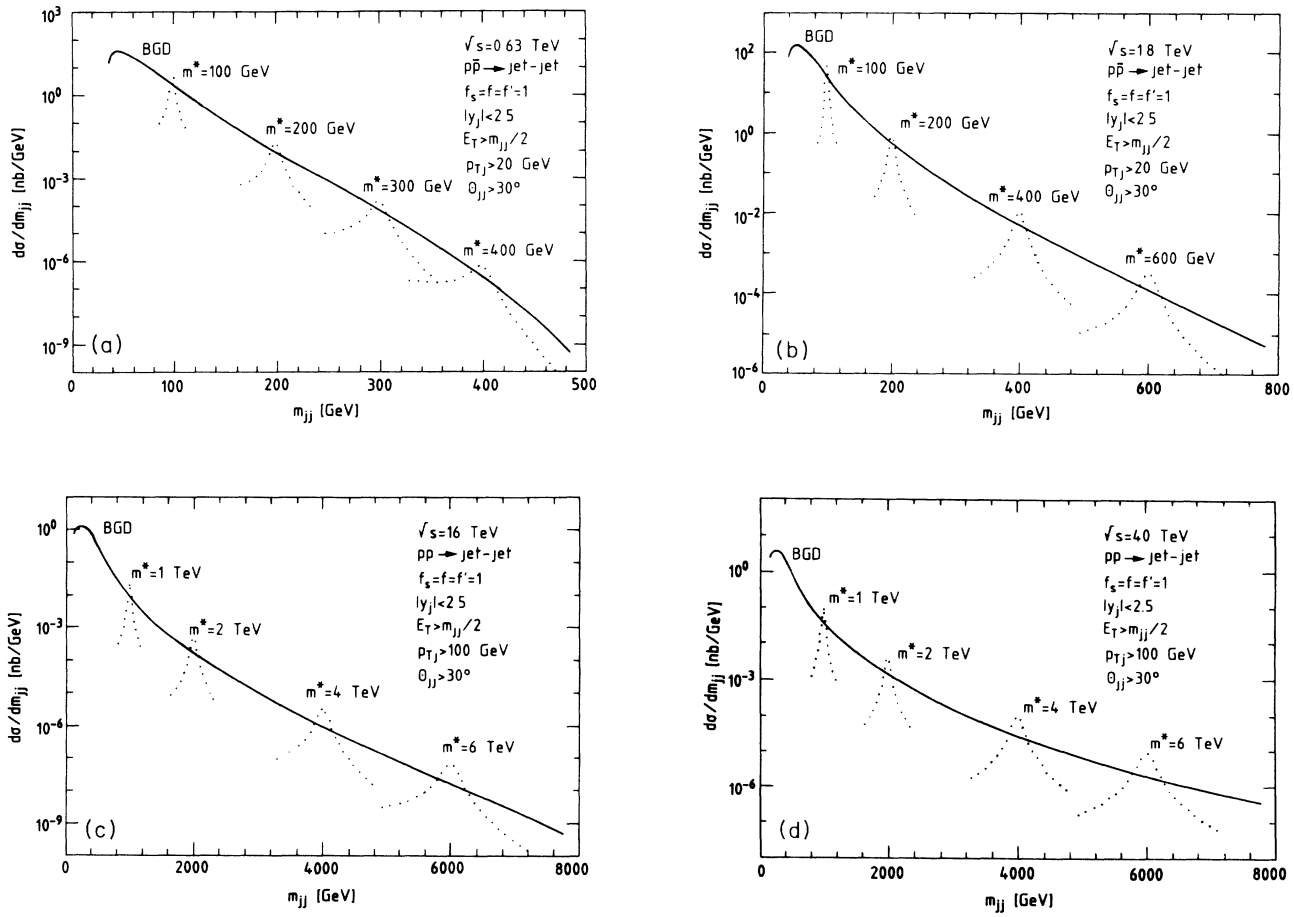

FIG. 3. Invariant-mass distributions $d\sigma/dm$ of excited quarks in the jj channel for various values of m^* (dotted lines) and (a) $p\bar{p}$ collisions at $\sqrt{s}=630$ GeV, (b) $p\bar{p}$ collisions at $\sqrt{s}=1.8$ TeV, (c) pp collisions at $\sqrt{s}=16$ TeV, and (d) pp collisions at $\sqrt{s}=40$ TeV. The solid curve represents the standard-model jj background.

simulate finite detector acceptances and to reduce the background, both jets are required to have rapidity $|y|<2.5$ and a transverse momentum $p_T>20$ GeV (100 GeV) for CERN collider and Fermilab Tevatron (LHC and SSC) energies. Furthermore a transverse energy cut $E_T>\frac{1}{2}m_{jj}$ is imposed. Finally, we demand a minimum opening angle of $\theta_{jj}>30°$ for the jets.

For CERN collider energies, the signal turns out to be only slightly larger than the QCD background [see Fig. 3(a)]. The signal-to-background ratio improves with m^* and $\sqrt{s}$ increasing, and at the SSC the q^* signal stands out clearly [see Fig. 3(d)]. A value different from one for $f_s=f=f'$ changes the width of the q^* resonance, but not its peak value. Similar results are obtained for $j\gamma$, jW, and jZ final states.[9] The total production cross section for

$$p\bar{p}(pp)\rightarrow q^*\rightarrow jj, j\gamma, jW, jZ \tag{14}$$

with $f_s=f=f'=1$, together with the estimate of the standard-model background, are shown in Figs. 4–7. To obtain the background cross sections we integrated the invariant-mass distribution of the background over twice the q^* width, assuming that gauge interactions dominate over contact interactions. This procedure, of course, is expected to result in a reliable estimate of the background only as long as the excited quark width is larger than the invariant-mass resolution of the detector in an actual experiment. The cuts imposed on the final-state particles in Figs. 4–7 are the same as those in Fig. 3, apart from the angular cut which we omitted for jW and jZ final states. It is obvious that in all channels the q^* production cross section is quite big and that the standard-model background should not pose serious problems in observing excited quarks. For $f_s=f=f'\neq 1$, the q^* production cross sections displayed in Figs. 4–7 have to be multiplied by a factor f_s^2. A parameter f_s of order m^*/Λ must explicitly be taken into account if m^* drops significantly below ~ 1 TeV.

So far we have assumed in this section that contact interactions do not significantly influence excited quark decays. The picture changes dramatically if the gauge in-

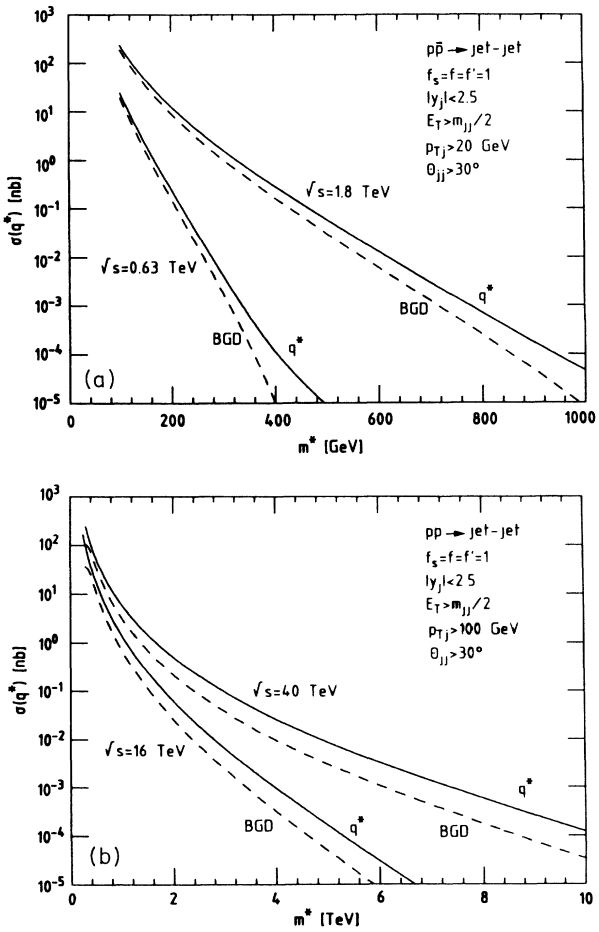

FIG. 4. (a) Cross sections for the production of excited quarks in $g+q\rightarrow q^*\rightarrow jj$ in $p\bar{p}$ collisions at $\sqrt{s}=630$ GeV and 1.8 TeV (solid lines). The dashed lines show the jj background from QCD. (b) Cross sections for the production of excited quarks in $g+q\rightarrow q^*\rightarrow jj$ in pp collisions at $\sqrt{s}=16$ TeV and 40 TeV (solid lines). The dashed lines show the jj background from QCD.

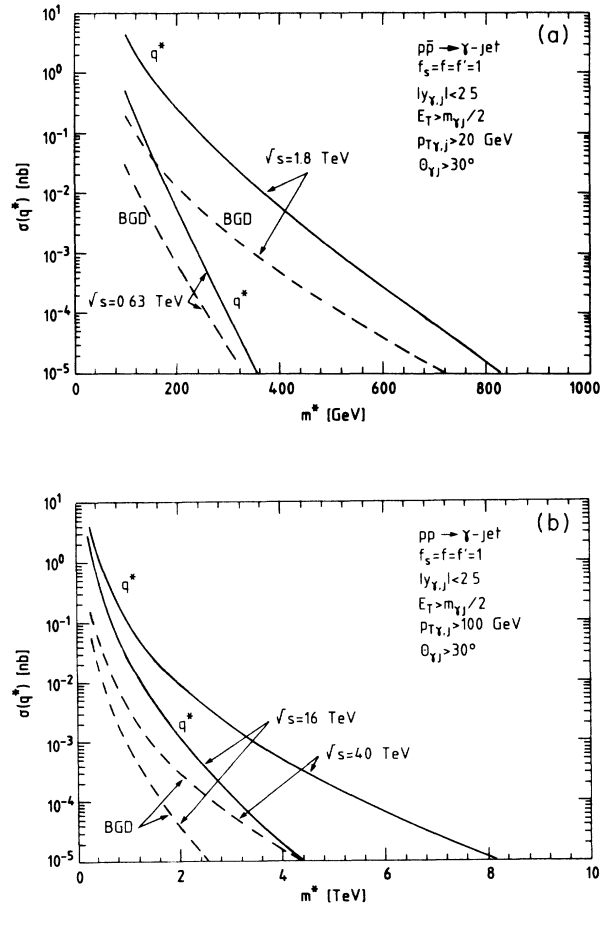

FIG. 5. (a) Cross sections for the production of excited quarks in $g+q\rightarrow q^*\rightarrow j\gamma$ in $p\bar{p}$ collisions at $\sqrt{s}=630$ GeV and 1.8 TeV (solid lines). The dashed lines show the standard-model $j\gamma$ background. (b) Cross sections for the production of excited quarks in $g+q\rightarrow q^*\rightarrow j\gamma$ in pp collisions at $\sqrt{s}=16$ TeV and 40 TeV (solid lines). The dashed lines show the standard-model $j\gamma$ background.

teractions are overwhelmed by contact interactions in the decay process. Excited quarks then decay mainly into jjj or jll final states. The main background source of three jet final states are quark-quark scattering processes with additional gluon bremsstrahlung or gluon induced three-quark final states where the quark interactions are dominated by contact terms. In contrast with the two-jet channel, the background dominates over the q^* signal in the jjj channel. This can easily be explained by noting that the phase-space restriction introduced by integrating the invariant-mass distribution of the jets over twice the q^* width allows for many more three-jet than two-parton combinations. Thus the three-jet background is larger than the two-jet background. The jll signal with a (non-resonant) lepton pair, on the other hand, is always much bigger than the standard-model lepton pair plus jet background and thus provides a clear signature in this case.

B. q^* production via contact interactions

If contact interactions contribute significantly to the decay rate of excited quarks they may also be important for q^* production at hadron colliders. Excited quarks can be produced through contact interactions in quark-quark collisions or in $q\bar{q}$ annihilation [see Fig. 2(b)], together with an ordinary quark. For purely left-handed currents in the effective Lagrangian Eq. (3) one obtains, for the parton cross sections,

$$\hat{\sigma}(qq' \to qq'^*) = \frac{\pi}{\hat{s}} \left[\frac{\hat{s}}{\Lambda^2} \right]^2 \left[1 - \frac{m^{*2}}{\hat{s}} \right]^2 , \tag{15}$$

$$\hat{\sigma}(qq \to qq^*) = \tfrac{8}{3} \hat{\sigma}(qq' \to qq'^*) \tag{16}$$

and

$$\hat{\sigma}(q\bar{q} \to q'\bar{q}'^*) = \frac{\pi}{4\hat{s}} \left[\frac{\hat{s}}{\Lambda^2} \right]^2 \left[1 + \frac{v}{3} \right] \times \left[1 - \frac{m^{*2}}{\hat{s}} \right]^2 \left[1 + \frac{m^{*2}}{\hat{s}} \right] , \tag{17}$$

$$\hat{\sigma}(q\bar{q}' \to q\bar{q}'^*) = \hat{\sigma}(q\bar{q} \to q'\bar{q}'^*) , \tag{18}$$

$$\hat{\sigma}(q\bar{q} \to q\bar{q}^*) = \tfrac{8}{3} \hat{\sigma}(q\bar{q} \to q'\bar{q}'^*) \tag{19}$$

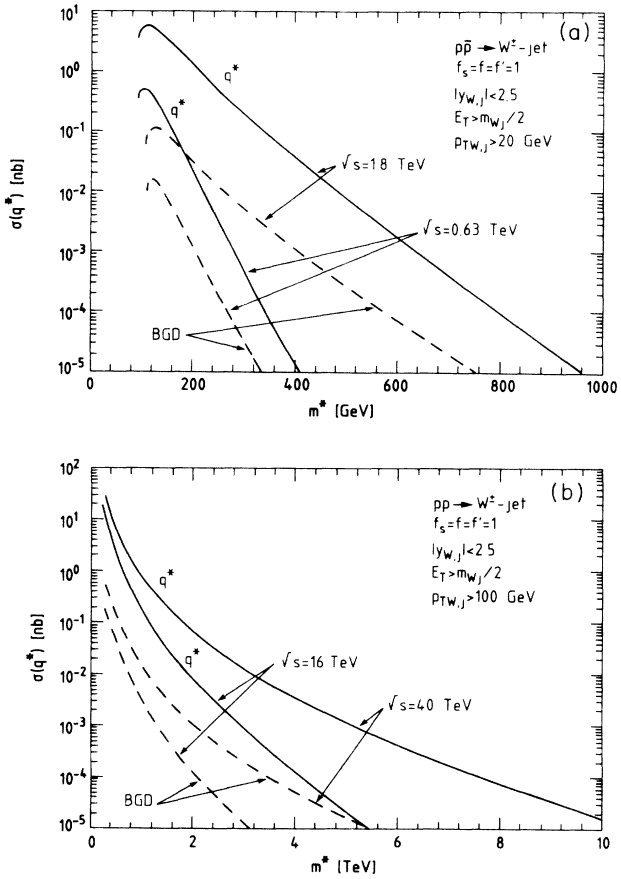

FIG. 6. (a) Cross sections for the production of excited quarks in $g+q \to q^* \to jW^{\pm}$ in $p\bar{p}$ collisions at $\sqrt{s}=630$ GeV and 1.8 TeV (solid lines). The dashed lines show the standard-model $jW^{\pm}$ background. (b) Cross sections for the production of excited quarks in $g+q \to q^* \to jW^{\pm}$ in pp collisions at $\sqrt{s}=16$ TeV and 40 TeV (solid lines). The dashed lines show the standard-model $jW^{\pm}$ background.

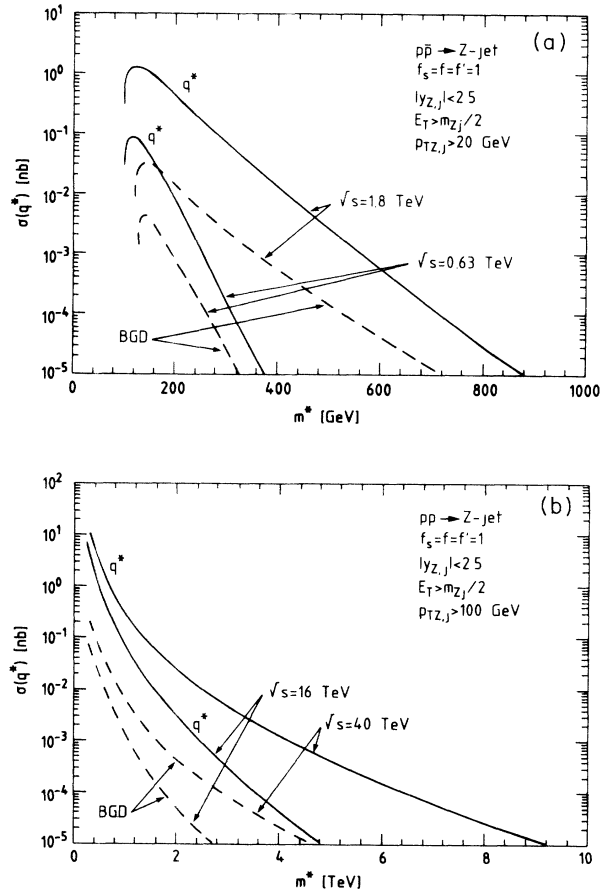

FIG. 7. (a) Cross sections for the production of excited quarks in $g+q \to q^* \to jZ$ in $p\bar{p}$ collisions at $\sqrt{s}=630$ GeV and 1.8 TeV (solid lines). The dashed lines show the standard-model jZ background. (b) Cross sections for the production of excited quarks in $g+q \to q^* \to jZ$ in pp collisions at $\sqrt{s}=16$ TeV and 40 TeV (solid lines). The dashed lines show the standard-model jZ background.

with

$$v=\frac{\hat{s}-m^{*2}}{\hat{s}+m^{*2}} \tag{20}$$

being the velocity of the q^* in the center-of-mass system of the subprocess. The validity of these expressions is limited to parton energies below Λ. Above this range, the growth of the parton cross section $\hat{\sigma}$ with $\hat{s}$ has to be damped by form factors. However, because the quark-quark luminosities fall rapidly with $\hat{s}$,[11] the damping does not affect the $p\bar{p}$ and pp cross sections significantly.

Excited quark decays, mediated either by gauge or contact interactions lead to final states consisting of three or four jets, two jets and a photon, or two jets and a lepton pair. Figure 8 shows the qq^* production cross sections for CERN collider, Fermilab Tevatron, LHC, and SSC energies and $m^*=\Lambda$ for q^* decays into three jets via contact interactions. The cuts imposed in Fig. 8 are the same as in Fig. 3, apart from the transverse energy for which we now require that $E_T > m^*$. To obtain the rates displayed in Fig. 8 we have summed over all possible q and q^* configurations. Comparison with Fig. 4 shows that, for the parameters chosen, the qq^* cross section is larger than the q^* production rate via quark-gluon fusion. Contact interactions may thus significantly enhance the production rate of excited quarks at hadron colliders. Details depend, of course, rather sensitively on the scale Λ; for $\Lambda \neq m^*$, the qq^* production rates shown in Fig. 8 have to be multiplied by a factor $(m^*/\Lambda)^4$.

The background to the qq^* signal with the q^* decaying into three jets via contact interactions consists of four-jet final states. The generic diagrams of the dominant mechanisms are shown in Fig. 9. In addition to pure QCD processes [Fig. 9(a)],[16] the contact interactions are the second most important source of four-jet background events [Fig. 9(b)]. These background cross sections (obtained by integrating the three-jet invariant mass over twice the q^* width) are significantly smaller than the signal, as demonstrated in Fig. 8. This is also the case for the background resulting from diagrams involving both QCD and contact interactions with gluons in the initial

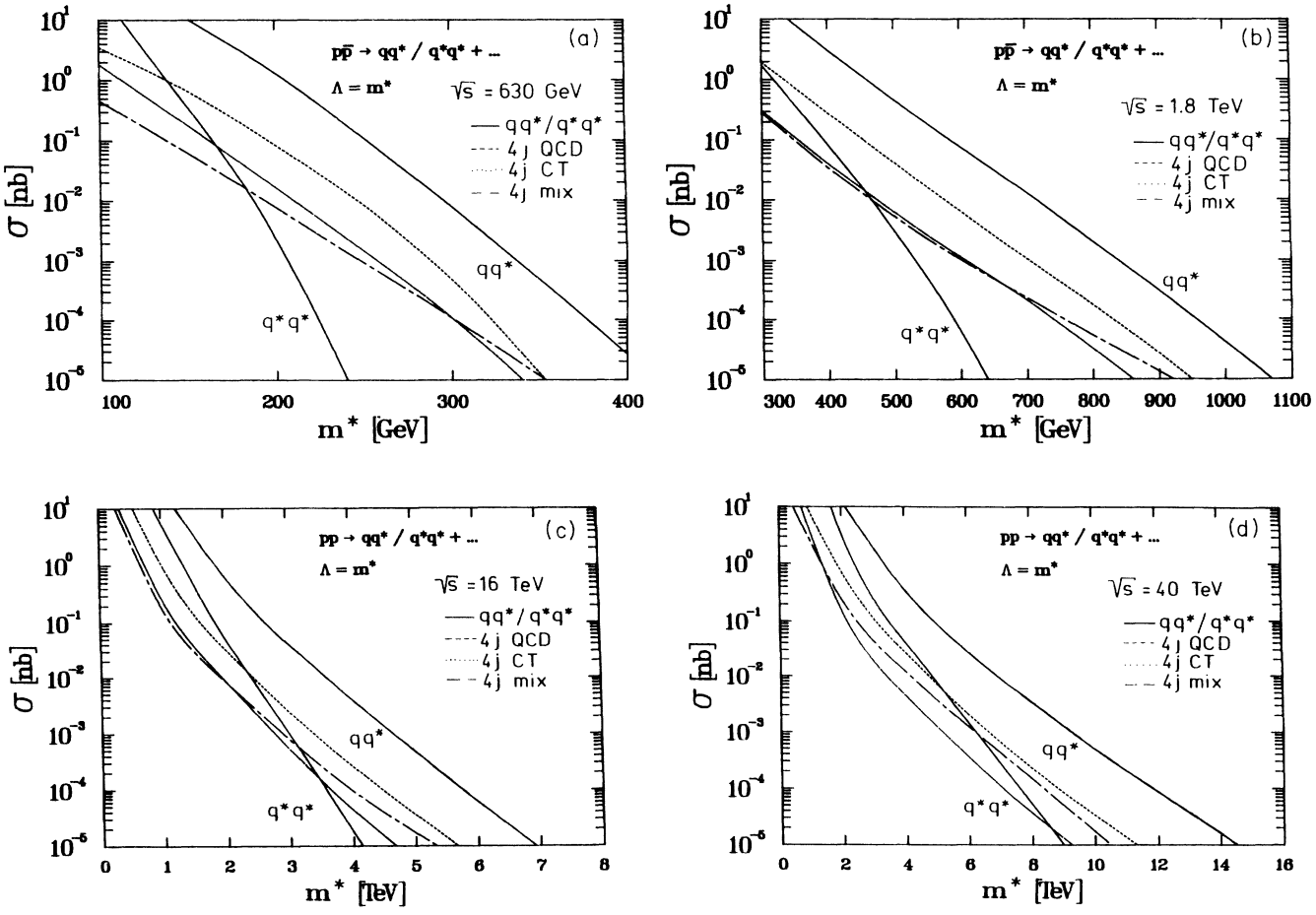

FIG. 8. (a) Cross sections for the associated production of ordinary and excited quarks in $p\bar{p}$ collisions at $\sqrt{s}=630$ GeV (solid line) with subsequent decay of the excited quark into three jets (via contact interactions). The dashed, dotted, and dashed-dotted lines show the four-jet background from QCD, contact interactions and diagrams involving both QCD and contact interactions. To calculate the four-jet background, the scale Q^2 used to evaluate α_s and the parton structure functions was chosen to be $E_T^2/4$. For comparison the cross sections for q^* pair production via contact interactions are included as well. (b) The same for $p\bar{p}$ collisions at $\sqrt{s}=1.8$ TeV. (c) The same for pp collisions at $\sqrt{s}=16$ TeV. (d) The same for pp collisions at $\sqrt{s}=40$ TeV.

or final state [see Fig. 9(c)].

Although the four-jet background is quite small, it will not be easy to discover excited quarks in the four-jet channel in an actual experiment. The q^* signal in this channel consists of a peak in the three-jet invariant-mass spectrum. Since one does not know which of the jets result from the q^* decay, a large combinatorial background arises from the wrong three-jet combination in the jjj mass distribution. This background will be of the same order as the signal and thus much larger than the four-jet background from QCD and contact interactions.

Contact interactions contribute also to the production of excited quark pairs [see Fig. 2(c)]. Since q^* pair production requires a larger center-of-mass energy than qq^* production, these processes are suppressed. For left-handed couplings in the contact interactions, one finds the parton cross sections

$$\hat{\sigma}(qq' \to q^* q'^*) = \frac{\pi \bar{v}}{\hat{s}} \left[\frac{\hat{s}}{\Lambda^2} \right]^2 \left[1 - \frac{2m^{*2}}{\hat{s}} \right], \tag{21}$$

$$\hat{\sigma}(qq \to q^* q^*) = \tfrac{1}{3} \hat{\sigma}(qq' \to q^* q'^*) \tag{22}$$

and

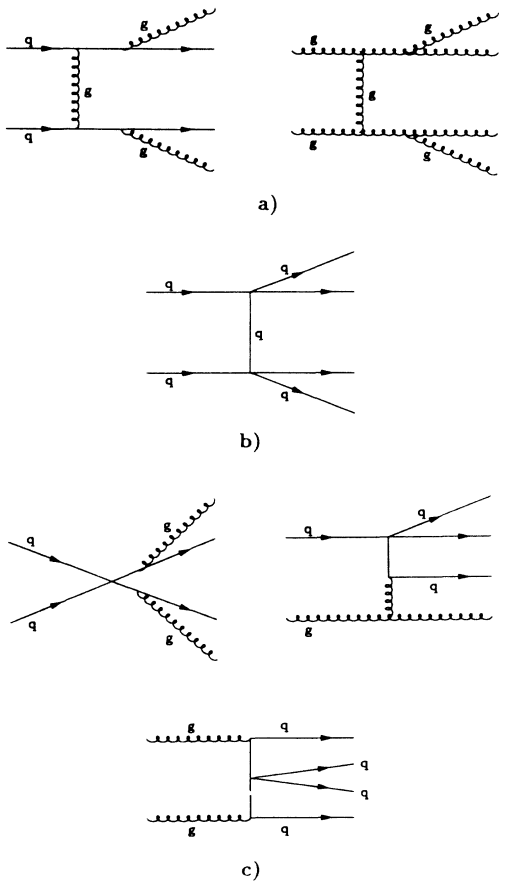

FIG. 9. Representative selection of Feynman diagrams contributing to four-jet production in hadronic collisions: (a) pure QCD subprocesses, (b) contact interactions, and (c) diagrams involving both QCD and contact interactions.

$$\hat{\sigma}(q\bar{q}' \to q^* \bar{q}'^*) = \frac{\pi \bar{v}}{3\hat{s}} \left[\frac{\hat{s}}{\Lambda^2} \right]^2 \left[1 - \frac{m^{*2}}{\hat{s}} \right], \tag{23}$$

$$\hat{\sigma}(q\bar{q} \to q'^* \bar{q}'^*) = \hat{\sigma}(q\bar{q}' \to q^* \bar{q}'^*), \tag{24}$$

$$\hat{\sigma}(q\bar{q} \to q^* \bar{q}^*) = \tfrac{8}{3} \hat{\sigma}(q\bar{q}' \to q^* \bar{q}'^*) \tag{25}$$

with

$$\bar{v} = \left[1 - 4\frac{m^{*2}}{\hat{s}} \right]^{1/2}. \tag{26}$$

The final states consist of jet bunches, e.g., $jjj + jjj$, and jets accompanied by gauge bosons or lepton pairs (e.g., $jll + jll$) for which the background from standard-model processes is small. The total q^* pair-production cross sections via contact interactions, summing over all possible q^* configurations, which result from Eqs. (21)–(25) with $\Lambda = m^*$, are also shown in Fig. 8. Similarly to the qq^* case, the q^* pair-production cross sections have to be scaled by a factor $(m^*/\Lambda)^4$ if $\Lambda \neq m^*$. Although these rates are substantially smaller than for qq^* production, they are still much larger than the cross sections for $q^*\bar{q}^*$ production via ordinary strong interactions,[11] unless $\Lambda \gg m^*$.

C. l^* production via contact interactions

The possibility to create leptons copiously through contact interactions in $p\bar{p}$ and pp collisions is one of the most exciting phenomena expected to occur in composite models in which quarks and leptons have common constituents.[11] In this case also excited leptons could be produced in large numbers either singly via $q\bar{q} \to l\bar{l}^*$, $l^*\bar{l}$, or pairwise via $q\bar{q} \to l^*\bar{l}^*$ ($l = e, \nu$). The parton cross sections, based on the effective Lagrangian of Eq. (3) with left-handed currents, are

$$\hat{\sigma}(q\bar{q} \to l\bar{l}^*, l^*\bar{l}) = \frac{\pi}{6\hat{s}} \left[\frac{\hat{s}}{\Lambda^2} \right]^2 \left[1 + \frac{v}{3} \right] \times \left[1 - \frac{m^{*2}}{\hat{s}} \right]^2 \left[1 + \frac{m^{*2}}{\hat{s}} \right], \tag{27}$$

and

$$\hat{\sigma}(q\bar{q} \to l^*\bar{l}^*) = \frac{\pi \bar{v}}{12\hat{s}} \left[\frac{\hat{s}}{\Lambda^2} \right]^2 \left[1 + \frac{\bar{v}^2}{3} \right]. \tag{28}$$

The total cross sections for single and pair production of excited electrons with $m^* = \Lambda$ at the CERN $p\bar{p}$ collider, the Fermilab Tevatron, the LHC and the SSC are shown in Fig. 10. Decays of excited leptons via gauge interactions lead to a lepton and a gauge boson while decays mediated by contact interactions give ljj or three-lepton final states. Associated production of ordinary and excited leptons thus yields final states consisting of two leptons plus a gauge boson, two leptons plus a jet pair, or four leptons. Pair production of excited leptons gives final states with up to six leptons. Background reactions to these channels are very rare in the standard model, and purely leptonic decays would provide very clear sig-

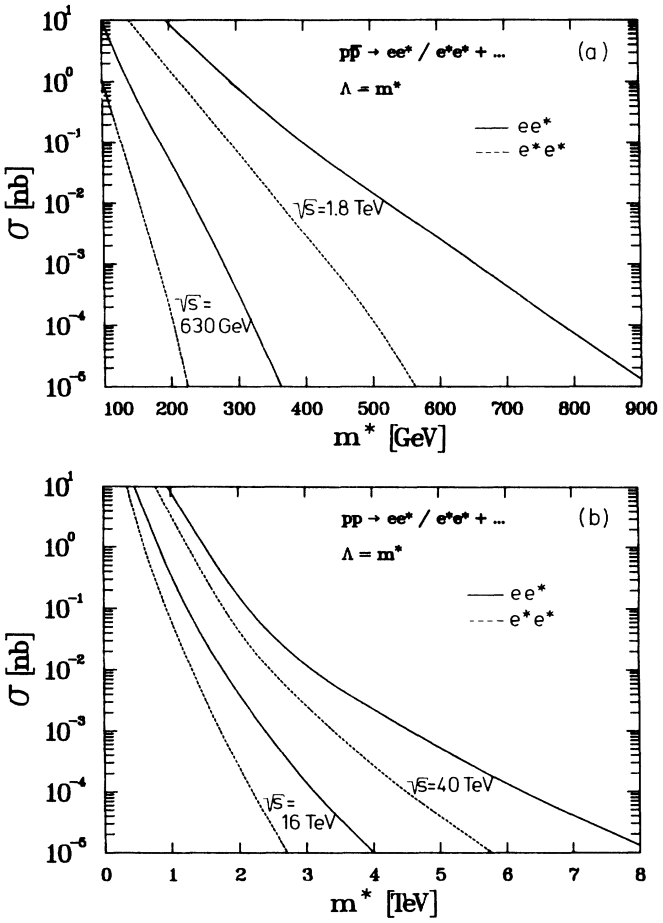

FIG. 10. (a) Cross sections for the associated production of ordinary and excited electrons (solid lines) and e^* pair production (dashed lines) in $p\bar{p}$ collisions at $\sqrt{s}=630$ GeV and 1.8 TeV. (b) Cross sections for the associated production of ordinary and excited electrons (solid lines) and e^* pair production (dashed lines) in pp collisions at $\sqrt{s}=16$ TeV and 40 TeV.

natures for the experimental identification of excited electrons.

V. CONCLUSIONS

As demonstrated above, excited quarks and leptons are produced with large cross sections in hadronic collisions. This observation can be condensed in a few numbers by deriving the maximum excited-quark and -lepton masses accessible at hadron colliders. As a discovery criterion we adopt the requirement that at least 100 signal events are observed within cuts. As before, the numbers are based on the assumption $m^*=\Lambda$, $f_s=f=f'=1$; with the cross sections given in the previous sections these numbers can easily be rescaled for any other choice of parameters. The discovery limits are summarized in Table IV. For the CERN collider (Fermilab Tevatron) an integrated luminosity $\int\mathcal{L}\,dt=6.6$ pb^{-1} (5 pb^{-1}), which corresponds to the presently available data sample, was assumed. For the SSC we took $\int\mathcal{L}\,dt=10^4$ pb^{-1} and for the LHC we considered two options: an integrated luminosity of 10^4 pb^{-1} and a "high luminosity" option[17] with $\int\mathcal{L}\,dt=4\times10^5$ pb^{-1}.

From Table IV we conclude that the limits which can be reached from qq^* production via contact interactions may well be of the same order, or even larger, as the bounds obtained from q^* production via quark gluon fusion. The maximum excited lepton masses which are accessible are somewhat smaller than the q^* masses one can probe. Details depend, of course, on the values chosen for Λ, f_s, f, and f'. While the presently operating $p\bar{p}$ colliders yield limits in the few hundred GeV range, it appears that, even if the parameters Λ, f_s, f, and f' are varied within large margins, LHC and SSC will *safely* reach the multi-TeV range on the subconstituent level. If $f_s=f=f'=0.1$, for example, the discovery limits for q^* production via gauge interactions would be about a factor 2 smaller than the numbers given in Table IV. Thus the larger value of the center-of-mass energies of the planned hadron supercolliders is directly reflected by the excited fermion discovery limits.

The discovery criterion upon which the numbers presented in Table IV are based, is, of course, very crude and does not include, e.g., the finite resolution of a detector in an actual experiment. Nevertheless, these discovery limits should correctly reflect the range of excited fermion masses one can probe with present and future hadron colliders.

In summary, hadron colliders turn out to be well suited for the search of excited quarks. Single q^* production may be much larger than $q^*\bar{q}^*$ production. Clean and simple experimental signatures with a small background are expected for excited quarks which are produced via qg fusion and decay via gauge interactions. Contact interactions may substantially enhance the q^* production cross section. This is reflected in the discovery limits for various hadron colliders summarized in Table IV. If quarks and leptons share common subconstituents, even excited leptons could be produced copiously at these machines, producing spectacular lepton final states.

TABLE IV. Maximum excited fermion mass m^* accessible at hadron colliders for $f_s=f=f'=1$ and $m^*=\Lambda$. Excited-fermion production via gauge (contact) interactions is labeled by [G] ([CT]).

$\int\mathcal{L}\,dt$	$Sp\bar{p}S$ 6.6 pb^{-1}	Fermilab Tevatron 5 pb^{-1}	LHC 10^4 pb^{-1}	LHC 4×10^5 pb^{-1}	SSC 10^4 pb^{-1}
q^* [G]	260 GeV	540 GeV	6.5 TeV	9.0 TeV	14 TeV
q^* [CT]	290 GeV	670 GeV	7.0 TeV	8.9 TeV	14.5 TeV
l^* [CT]	220 GeV	480 GeV	4.0 TeV	5.6 TeV	8.2 TeV

ACKNOWLEDGMENTS

We are grateful to D. Zeppenfeld for useful discussions and for carefully reading the manuscript. P.Z. would like to thank J. Ellis for a stay at the CERN TH Division while part of this work was being done. This research was supported in part by the University of Wisconsin Research Committee with funds granted by the Wisconsin Alumni Research Foundation, and in part by the U.S. Department of Energy under Contract No. DE-AC02-76ER00881. This work was supported in part by the West German Bundesministerium für Forschung und Technologie.

[1]F. Low, Phys. Rev. Lett. **15**, 900 (1965).

[2]F. M. Renard, Phys. Lett. **116B**, 264 (1982); **139B**, 449 (1984).

[3]N. Cabibbo, L. Maiani, and Y. Srivastava, Phys. Lett. **139B**, 459 (1984).

[4]A. De Rújula, L. Maiani, and R. Petronzio, Phys. Lett. **140B**, 253 (1984).

[5]J. Kühn and P. Zerwas, Phys. Lett. **147B**, 189 (1984).

[6]J. Kühn, H. D. Tholl, and P. Zerwas, Phys. Lett. **158B**, 270 (1985).

[7]K. Hagiwara, S. Komamiya, and D. Zeppenfeld, Z. Phys. C **29**, 115 (1985).

[8]R. Kleiss and P. Zerwas, in *Proceedings of the Workshop on Physics at Future Accelerators,* La Thuile, Italy, 1987, edited by J. H. Mulvey (CERN Report No. 87-07, Geneva, Switzerland, 1987).

[9]U. Baur, I. Hinchliffe, and D. Zeppenfeld, in *From Colliders to Supercolliders,* proceedings of the Workshop, Madison, Wisconsin, 1987, edited by V. Barger and F. Halzen [Int. J. Mod. Phys. A **2**, 1285 (1987)].

[10]I. Bars and I. Hinchliffe, Phys. Rev. D **33**, 704 (1986).

[11]E. Eichten, I. Hinchliffe, K. Lane, and C. Quigg, Rev. Mod. Phys. **56**, 579 (1984).

[12]T. Kamae, in *Proceedings of the XXIV International Conference on High Energy Physics,* Munich, West Germany, 1988, edited by R. Kotthaus and J. H. Kühn (Springer, Berlin, 1988), and references therein.

[13]M. Spira and P. M. Zerwas, in Proceedings of the 7th INFN Eloisatron Project Workshop, Erice, Italy, 1988 (unpublished).

[14]M. S. Chanowitz and S. D. Drell, Phys. Rev. Lett. **30**, 807 (1973).

[15]G. B. West and P. Zerwas, Phys. Rev. D **10**, 2130 (1974).

[16]Z. Kunszt, Nucl. Phys. **B247**, 339 (1984); and (private communication); Phys. Lett. **145B**, 132 (1984); Z. Kunszt and W. J. Stirling, Phys. Lett. B **171**, 307 (1986).

[17]J. H. Mulvey, Report No. CERN 88-02, 1988 (unpublished).